

Two high-throughput technologies to detect segmental aneuploidies identify new Williams-Beuren Syndrome patients with atypical deletions

Cédric Howald^{1,9}, Giuseppe Merla^{1,2,9}, Maria Cristina Digilio³, Styliani Amenta⁴, Robert Lyle¹, Samuel Deutsch¹, Urmila Choudhury^{1,5}, Armand Bottani⁶, Stylianos E. Antonarakis^{1,6}, Helen Fryssira⁴, Bruno Dallapiccola^{2,7} and Alexandre Reymond^{1,8,*}

¹Department of Genetic Medicine and Development, University of Geneva Medical School, Geneva, Switzerland

²Medical Genetics Unit, IRCCS "Casa Sollievo della Sofferenza", San Giovanni Rotondo, Italy

³Medical Genetics Unit, IRCCS "Bambino Gesù" Hospital, Rome, Italy

⁴Department of Medical Genetics, Athens University School of Medicine, Aghia Sofia Children's Hospital, Athens, Greece

⁵NCCR Frontiers in Genetics graduate program, University of Geneva, Geneva, Switzerland

⁶Division of Medical Genetics, Geneva University Hospitals, Geneva, Switzerland

⁷C.S.S.-Mendel Institute, Roma, Italy

⁸Center for Integrative Genomics, University of Lausanne, Lausanne, Switzerland

⁹These authors contributed equally to this work.

*corresponding author

Alexandre Reymond, Center for Integrative Genomics, University of Lausanne, Lausanne, Switzerland, PH 00 41 21 692 3960, FX 00 41 21 692 3965,

EM alexandre.reymond@unil.ch

Abstract

Introduction

We developed and compared two new technologies to diagnose a contiguous gene syndrome, the Williams-Beuren syndrome (WBS).

Methods

The first proposed method, named Paralogous Sequence Quantification (PSQ), is based on the use of paralogous sequences located on different chromosomes and quantification of specific mismatches present at these loci using the Pyrosequencing technology. The second exploits quantitative real-time PCR (QPCR) to assess the relative quantity of an analyzed locus.

Results

A correct and unambiguous diagnosis was obtained for 100% of the analyzed samples with either techniques (n=165 and n=155, respectively). These methods allowed the identification of two patients with atypical deletions in our cohort of 182 WBS patients.

Conclusions

We conclude that both PSQ and QPCR are robust, easy to interpret and simple to set-up methods to diagnose segmental aneuploidies, thus representing a competitive alternative for widespread use in diagnostic laboratories. These methods have advantages over Fluorescence *in situ* Hybridization or microsatellites/SNP genotyping for detecting short segmental aneuploidies since the former is costly and labor intensive and the latter dependent on informativeness of the polymorphisms. Both patients with atypical deletions presented mild facial anomalies, mild mental retardation with impaired visuo-spatial cognition, supraaortic stenosis and normal growth parameters. These observations are consistent with the involvement of GTF2IRD1 and/or GTF2I in some of the WBS facial features.

Keywords

Williams-Beuren syndrome, aneuploidy, diagnosis, genomics, real-time PCR, pyrosequencing

Introduction

An increasing number of human diseases are recognized to result from recurrent DNA rearrangements involving unstable genomic regions. Both inter- and intrachromosomal rearrangements are facilitated by the presence of region-specific Low-Copy Repeats (LCRs) and result from nonallelic homologous recombination. These diseases are traditionally diagnosed by FISH (Fluorescence *in situ* Hybridization)¹ and/or microsatellite/SNP genotyping². FISH has the disadvantages of being labor intensive and expensive, whereas microsatellite/SNP genotyping depends on the relative informativeness of the polymorphisms used and on parental DNA to ascertain the deletion.

The completion of the human genome sequence³⁻⁵ has provided an extensive catalog of sequence features that can be exploited for the design of new diagnostic strategies. Here we propose and validate two recently described PCR-based diagnostic approaches to identify contiguous gene syndromes. We compare their efficiency and practicality to detect the 7q11.23 microdeletion in Williams-Beuren Syndrome (WBS) patients⁶. WBS has a prevalence estimated between 1/7500 and 1/20000⁷⁻⁹. Patients are characterized by mental retardation with unique cognitive and personality profile, distinctive facial features, supravalvular aortic stenosis, short stature, connective tissue anomalies, hypertension, infantile hypercalcemia, dental and kidney abnormalities, premature aging of the skin, impaired glucose tolerance and silent diabetes¹⁰⁻¹².

The first method is based on the use of paralogous sequences located on different chromosomes. Because these sequences are under different selective constraint, they accumulate nucleotide substitutions in a locus specific manner. Thus each locus will contain specific internal sequence differences (Paralogous Sequence Mismatches or PSMs), which can be exploited to estimate their relative quantity. Technically, we co-amplify paralogous fragments of identical size that map to different autosomes and quantify the PSMs to detect the presence of chromosome number abnormalities. This technology, named Paralogous Sequences Quantification (PSQ) was recently successfully implemented to detect autosomal trisomies, as well as numerical abnormalities of sex chromosomes¹³.

The second methodology, real-time Quantitative Polymerase Chain Reaction (QPCR), allows detection of a PCR product as it accumulates during the reaction^{14, 15}. The higher the copy number of a target sequence, the earlier a significant increase in fluorescence will be detected. We can thus estimate the relative quantity of an analyzed locus. By designing multiple assays within and next to a segmental aneuploidy, we should be able to map exactly the extension of an indel. We report the implementation of these technologies to diagnose WBS and to map the breakpoints of atypical rearrangements.

Materials and Methods

Samples

Samples were collected by the C.S.S.-Mendel Institute, Roma (140 Italian WBS patients and 43 Italian controls), the Aghia Sofia Children's Hospital, Athens (31 Greek WBS patients) and the Department of Genetic Medicine and Development, University of Geneva, Geneva (34 French controls from the Departments of Savoie and Haute-Savoie, 11 WBS patients and 15 controls from Western Switzerland) with appropriate informed consent obtained by the physician in charge and approval of the local ethical committee. Genomic DNA was prepared with either the PUREGENE whole blood kit (Gentra Systems) or the QIAamp kit (Qiagen).

Paralogous sequence quantification and pyrosequencing

Paralogous sequence quantification and pyrosequencing were performed as described¹³. The forward and reverse primers and the internal sequencing primers were designed using Oligo 6.55 (Molecular Biology Insights) and the manufacturer's site (<http://www.pyrosequencing.com/index.html>), respectively. Reverse and sequencing primers were desalted, while the biotinylated forward primers were desalted and purified by HPLC (Sigma-Genosys). PCR reactions with the selected primer pairs (Table S1) were set up in a total volume of 25 µl containing 30 ng of genomic DNA, 400 µM of each primer and 200 µM dNTPs. We used 1.25 units of a standard *Taq* polymerase in the manufacturer provided buffer (Amersham Biosciences), or alternatively the ready made 2xJumpstart PCR mastermix (Sigma-Genosys) with varying levels of MgCl₂ and DMSO depending on the assay (Table S1). Three negative controls per plate were added and the PCR products were checked on agarose gel to ensure lack of PCR contamination and correct amplicon size. PCR products were purified, and annealed to an internal sequencing primer close to the PSM site to be quantified (Table S1; Figures S1-S2). The purification and pyrosequencing steps were performed following the instructions of the manufacturer (Biotage). The Pyrosequencing software directly outputs a quantitative value for the proportion of each PSM present in the PCR product (Figure S3). We used the relative abundance of the PSM of the 'query' chromosome as our statistic for all calculations. The methods used to determine the PSM relative abundance that could be confidently diagnosed (99% confidence interval), the sensitivity and the specificity of each assay and to combine assays were described in¹³.

Real-time quantitative PCR

Oligos were designed using the PrimerExpress program (Applied Biosystem) with default parameters in every case (Table S2) and ordered from Sigma-Genosys. Amplicon sequences were checked by both BLAST and BLAT against the human genome to ensure specificity. All RT-PCR reactions were performed in two replicates in 9 µl final volume with concentration of 0.96 ng/µl of DNA, 0.42 µM of each primer and 1xSybrGreen mastermix (Applied Biosystems). Reactions were set up in a 384 wells plate format with a Biomek 2000 (Beckman) and run in an ABI Prism7900HT (Applied Biosystems) with the following amplification conditions: 50°C for 2 min, 95°C for 10 min, and 50 cycles of 95°C 15 sec/60°C 1 min. Raw Ct values were obtained using SDS2.0 (Applied Biosystems). We implemented the geNorm method¹⁶ to measure relative quantities. Four normalization assays mapping to HSA21 (Table S2) and four normalization DNAs were systematically included in each run.

Results

Paralogous sequence quantification

Paralogous sequences were identified by comparing 10 kb-long fragments covering the WBS deletion¹⁷ with the human genome sequence using both BLAT (<http://genome.ucsc.edu/>) and BLAST (<http://www.ensembl.org/Multi/blastview>). We identified two pairs of suitable paralogous sequences with one copy to chromosome 7q11.23 and only a single second copy elsewhere in the genome (Figures S1-S2). We aligned all matching sequences, and built a consensus sequence to design three discriminating Pyrosequencing assays (assay BAZ1B and assays CYLN2 and WBS3.4M, respectively) for WBS deletion detection. Each assay was tested with a number of PCR conditions on 10 control and 10 WBS samples. From this analysis we selected the conditions based on the following criteria: (i) the Paralogous Sequence Mismatches (PSM) quantification in control individuals should be close to 50%/50%, indicating that both 'loci' amplify with equal efficiency; and (ii) there should be a clear, non-overlapping discrimination between control and WBS samples. For the CYLN2

and WBSR3.4M assays we found conditions that showed PSM relative abundances close to the theoretical values of 50%/50% for control individuals and 66%/33% for patients (Table S1). In contrast for the BAZ1B assay, and despite testing multiple triads of amplification and sequencing primers (data not shown), we were unable to identify conditions that produced PSM relative abundances close to the theoretical values.

To validate the method on a larger cohort, we tested 128 WBS patient, 16 probably WBS patient (see below) and 37 control samples collected by the C.S.S.-Mendel Institute. Typical results and distribution of PSM relative abundance of normal and affected samples for each assay are shown in Figure S3. We use the relative abundance of the PSM from the “query” chromosome, i.e. the chromosome we want to quantify, here HSA7, as our statistic for all calculations. For both the CYLN2 and the WBSR3.4M assay, the distribution of the ‘query’ chromosome PSM relative abundance obtained for both cohorts show normal distributions with medians close to the expected results of 33% for WBS patients (CYLN2 relative abundance: mean=33±2%; WBSR3.4M:37±2%) and 50% for control individuals (CYLN2:47±2%; WBSR3.4M:50±2)(see Table 1). The third assay recorded relative abundances of the ‘query’ chromosome PSM under the expected value for both the controls and the patients samples (mean=41±6, range 39-47% and 27±5%, 12-44%, respectively) and 3% of misdiagnoses (n=160). It was therefore not retained further.

Both retained assays were characterized by no false negative or false positive calls, but some samples fell outside of the 99% confidence interval and could therefore not be unambiguously diagnosed. They were treated either as false positives or as false negatives according to the known FISH result to estimate sensitivity and specificity (Table 1). Combination of both assays resulted in a clearer separation between the control and the patient samples (Figure 1) and a significant improvement of the sensitivity (Table 1).

Table 1 Specificity and Sensitivity of PSQ assays

Assay	CYLN2	WBSR3.4M	Combined
Mean control	46.7	50.3	50.0
SD control	1.9	2.2	1.6
Mean WBS	32.9	37.3	36.1
SD WBS	2.2	1.7	1.6
Number of samples	163	160	160
Number of uncertain samples	6	4	3
Sensitivity	0.95	0.97	0.98
Specificity	1.00	1.00	1.00

Six subjects of the “probably WBS” cohort, that were clinically diagnosed as WBS but were not analyzed by FISH and /or Southern, showed “query” chromosome relative abundance that classified them in the 99% confidence interval of the control cohort with all three assays (not shown). Consistently, for two of these patients there was only a suspicion of WBS, while a third showed facial features, but no other characteristic phenotypes that can be attributed to this disease (see below).

Quantitative real-time PCR

A quantitative real-time PCR (QPCR) method has been recently successfully implemented to diagnose aneuploid mice¹⁸. To assess if the technology could be used to diagnose human segmental aneuploidies and to evaluate its qualities/disadvantages vs. the PSQ technology, we applied this second high-throughput technology to diagnose the WBS segmental aneuploidy. Moreover, implementation of this second procedure should allow to clarify ambiguous cases

and atypical deletions and, eventually, exactly map the breakpoints of unusual rearrangements.

We designed 20 QPCR assays spread from HSA7 bp 70012994 to bp 75057642 (Table S2) and preliminarily tested them on DNAs from four controls and three WBS patients. A set of 11 assays were retained and used to analyze 94 WBS patients, 16 probably WBS and 61 controls collected by the C.S.S.-Mendel Institute (55 WBS, 16 probably WBS, 14 controls), the Department of Genetic Medicine, Geneva (8 patients, 47 controls) and the Aghia Sofia Children’s Hospital, Athens (31 patients). These assays map either centromerically (2 assays), inside (6) or telomerically (2) to the commonly deleted region. A further assay, named 4_WBSCR16, maps between the two blocks of repeats that flank the telomeric side of the WBS critical region inside the WBSCR16 gene¹⁹. Mean results and typical examples are presented in Figures 2 and S4, respectively. These assays show mean results close to the expected value of 1 for controls. Consistently, the mean results obtained with the patients samples are close to 1 for assays outside the common deletion and to 0.5 for assays inside the deletion (Table 2). All six diagnostic assays showed no false negative or false positive calls, but a few samples (0.7 to 4.6%) fell outside of the 99% confidence intervals for one (12 samples), three (2 samples) or even four assays (1 sample; Table 2). However even these samples can be unambiguously diagnosed upon combination of the six assays (pairwise t-test: all individual p values <0.0016, n=153, atypical deletions not included, see Table 2). To further validate this method, we performed a blind test on 24 DNAs collected by the Department of Genetic Medicine, Geneva and previously analyzed by FISH. We confirmed the clinical diagnosis of WBS (11 cases) and normals (15 cases) for the 7q11.23 region in all cases (all individual p values <0.0009).

Table 2 Specificity and Sensitivity of QPCR assays

Assay	20_O8N8C3	19_WBSCR17	17_BAZ1B	15_TBL2	14_WBSCR14	9_ELN	6_RFC2	5_CYLN2	4_WBSCR16	3_HIP1	2_CCL26	6 Dx assays Combined
Mean control	1.01	1.06	0.81	1.06	1.04	0.99	1.04	0.98	0.91	0.86	1.07	0.99
SD control	0.12	0.09	0.10	0.11	0.12	0.10	0.11	0.10	0.09	0.12	0.12	0.13
Mean WBS	1.07	1.02	0.43	0.51	0.53	0.48	0.51	0.48	0.92	0.86	1.09	0.49
SD WBS	0.18	0.13	0.11	0.06	0.07	0.05	0.06	0.06	0.12	0.18	0.13	0.08
Number of samples	153	153	152	153	153	152	152	152	153	153	153	153
Number of uncertain samples			2	2	1	7	4	6				0
Sensitivity			0.98	0.99	0.99	0.96	0.97	0.96				1.00
Specificity			1.00	0.98	1.00	0.96	0.98	0.97				1.00

The six patients of the “probably WBS” group, that exhibit PSM relative abundancies placing them in the control group (see above), showed no evidence of deletion in the 7q11.23 region with the QPCR method either (combination of 6 diagnostic assays, pairwise t-test: all individuals p values <0.006). Thus the results obtained with the two independent methods (PSQ and QPCR) are consistent with the interpretation that these six patients were clinically misdiagnosed. Since no FISH and/or Southern blot results were available for them, we considered that they were clinically misdiagnosed and reclassified them as non-WBS. However, we cannot exclude that these individuals carry an inversion or a subtle deletion, that maps between the assays we used (maximum size 415 kb between WBSCR14 and ELN).

Atypical deletions

Two patients, CO3 and IM3, present an atypical deletion on the telomeric side as measured by both PSQ and QPCR. Their DNAs contain one copy of the BAZ1B (diagnosed with PSQ and QPCR), TBL2 (QPCR), ELN (QPCR) and RFC2 (QPCR) loci, but are unaffected at the WBSCR3.4M (PSQ) and CYLN2 (PSQ and QPCR) assays (Figures 1 and 3). To further narrow down the breakpoints, we designed more QPCR assays between RFC2 and CYLN2 (Table S2). These additional assays allowed mapping the CO3 and IM3 breakpoints to 13011

and 66180 bp long intervals, respectively. Thus these patients present atypical deletions smaller by more than 400 kb, when compared to the extent of the classical WBS deletion (Figure 3)¹⁷. The breakpoints of IM3 and CO3 map in the region between the RFC2 and CYLN2 genes. All the WBS genes centromerically positioned from this point, starting with the RFC2 gene, are deleted, while the two telomeric genes, GTF2IRD1 and GTF2I, are preserved. The situation is more ambiguous for the CYLN2 gene. 12.3 to 25.3 kb separate the mapped CO3 breakpoint from the first known exon of CYLN2. Similarly, the IM3 breakpoint was narrowed down to a region that encompasses the promoter and the three first exons of that gene. Thus both cases display genomic organizations that might impair the normal expression of CYLN2.

Patient CO3, a male, was born by vaginal delivery after an uneventful pregnancy of 32 weeks. Birth weight was 1850 gr (P50-P75), length 43 cm (P50), and head circumference 29 cm (P25). Congenital heart defect was diagnosed at 5 months of age and echocardiography revealed a supravalvular aortic stenosis. Patient IM3, a female, was born by vaginal delivery at term of an uneventful pregnancy. Birth weight was 3100 g, length 49 cm and head circumference 34 cm. Congenital heart defect was diagnosed shortly after birth. Echocardiography showed supravalvular aortic and peripheral pulmonary arteries stenoses that were surgically corrected at 5 years. Both patients showed motor developmental milestones in the normal range, though mild cognitive deficit was evident at 4 years in one patient (CO3). CO3 and IM3 showed difficulties in non-linguistic and visual-motor abilities, overfriendliness and preservation of linguistic abilities. Wechsler Intelligence Scale testing performed at 15 and 10 years of age showed mild mental retardation with IQs of 72 (VIQ 74; PIQ 68) and 71 (VIQ 73; PIQ 66), respectively. Their clinical examination showed mild facial anomalies, including periorbital fullness (mild in CO3) and thick lower lip, normal size and number of teeth and blood glucose levels in the average range.

CO3 is now 30 years old; weight is 77 kg (P90-P97), height 168 cm (P10), head circumference 53 cm (P3). His irises are normal and no signs of premature ageing were noticeable. Ophthalmological and audiological evaluations were normal. Renal ultrasonography showed no malformations. Measurements of blood pressure at rest and during 24-hour ambulatory monitoring were in the normal range. Auxological parameters of IM3 at 11 years of age were normal. Weight was 38,5 kg (P50-P75), height 140 cm (P50), head circumference 50 cm (P3). She presented a hoarse voice, a stellate iris and mild malar hypoplasia. Strabismus was operated at 7 years of age. Audiological evaluation and renal ultrasonography were normal. Measurements of blood pressure at rest and during 24-hour ambulatory monitoring showed mild systolic hypertension.

Discussion

We report the setup and validation of two recently described methods to diagnose the recurrent DNA deletion present in Williams-Beuren syndrome (WBS) patients^{6, 17}. The first technique, called Paralogous Sequence Quantification (PSQ), is based on the quantification of two paralogous sequences by pyrosequencing^{13, 20}. PSQ allowed us to correctly segregate 161 of the 163 tested samples with no false positives and/or false positive calls. The diagnosis of the remaining two samples was inconclusive as they fell outside of the confidence interval of the combined assay (Table 1). We conclude that the PSQ technology is a reliable, effective and inexpensive tool to diagnose segmental aneuploidies, but that it is not suitable to measure the extent of the deletion in the case of WBS for the lack of exploitable paralogous sequences at the centromeric end of the deletion.

The second method takes advantage of quantitative real time PCR to evaluate relative abundance of a DNA fragment. We designed a set of eleven assays mapping to the 7q11.23 region and tested them on 92 WBS patient and 61 control DNAs. They allowed the correct segregation of the two analyzed cohorts in all of the tested genomes with 100% sensitivity and specificity (Table 2).

The PSQ method is less expensive than the QPCR technology to diagnose segmental aneuploidies. However, PSQ has the weakness to be dependent on the presence of suitable sequences, i.e. sequences paralogous to sequences somewhere else on the genome. This is not a major problem when the goal is to diagnose aneuploidies of entire chromosome or large chromosomal region¹³, but it becomes important in partial aneuploidies of small size (<5Mb) like WBS. In contrast, assays for the QPCR technology can be designed on any genomic fragment that is uniquely represented in the human genome. This allows designing a large number of assays along the region to be tested, e.g. a segmental aneuploidy, decreasing the risk of false positives and negatives and increasing the resolution. Moreover, atypical indels can then be characterized further by designing more assays close to the supposed breakpoints, as we did to characterize WBS patients that carry two copies of the CYLN2, GTF2IRD1 and GTF2I genes.

Genetic diagnostic laboratories attached to genetic counseling clinics, routinely use FISH, microsatellite/SNP genotyping and/or Southern to diagnose segmental aneuploidies, including the Williams-Beuren syndrome. FISH and Southern have success rates reaching 99%, but they have the disadvantage of being costly and labor intensive. Microsatellite/SNP genotyping requires the analysis of multiple assays of both the proband and his/her parents to ensure the informativeness of the genotyped polymorphisms. Another drawback inherent to this method is the unwanted prospect of identifying non-paternities. Advantages and disadvantages of these different methods to diagnose segmental aneuploidies are summarized in Table 3.

Table 3: Advantages and Disadvantages of the multiple techniques used to diagnose segmental aneuploidies

	Method				
	QPCR	PSQ	FISH	Microsatellites	Southern
speed [day]	1	1	5 (2) ¹	1	6
cost/assay [€]	30	10	80	15/30/45 ^{2,3}	80
advantages	great adaptability to uncommon rearrangement ⁴		possibility to diagnose inversion ⁵		possibility to diagnose inversion
disadvantages	impossibility to diagnose inversion	relies on paralogous sequences impossibility to diagnose inversion	labor intensive	relative informativeness of SNPs discovery of non-paternity impossibility to diagnose inversion	requires to work with radioactivity ⁶ labor intensive

¹a preliminary results can be given after 2 days

²price for QF-PCR

³45€/assay includes both parents

⁴see for example the mapping of breakpoints of atypical deletion patient detailed in this report

⁵by 3 color FISH (see for example Osborne et al., 2001)

⁶possibility to work with non-radioactive DIG, but with a diminished sensitivity

We further report the detection of two patients, who carry partial deletions that do not extend telomerically further than the RFC2 gene (Figure 3). The status of the relative expression of the neighboring CYLN2 gene remains uncertain, as we can hypothesize that the hemizyosity of the sequences preceding that gene might play an important role in the regulation of its expression. These atypical patients can provide important information for genotype and phenotype correlation. A few WBS individuals with atypical deletion as well as patients with isolated SVAS and partial deletions were previously identified²¹⁻²⁹. In particular an individual who carried an atypical deletion extending from the centromeric LCR to the CYLN2 or the GTF2IRD1 gene (Figure 3C) and presented an unusual cognitive profile, SVAS, milder facial features, short stature and an IQ of 83, but not the specific visuospatial impairment of WBS patients was reported²³. Likewise,²⁷ describes a seven-year-old female with a deletion from the centromeric LCR to RFC2 (status of CYLN2 unclear; Figure 3B) with no dysmorphic features and verbal and performance scores slightly above full deletion WBS. In addition, a Japanese patient with a deletion spanning most of the WBS region with the exception of GTF2IRD1 and GTF2I had abilities to visualize at the spatial and at the global levels that outperformed that of typical WBS despite a VSIQ of 64²²(Figure 3B). Finally, the affected members of a SVAS kindred without typical Williams facies and visual spatial abilities above that of full deletion WBS were shown to carry smaller deletion from ELN to GTF2IRD1 thus maintaining euploidy of GTF2I²⁸(Figure 3B). These combined observations allowed to suggest that the GTF2I and/or GTF2IRD1 genes are likely to be linked to the characteristic WBS visual spatial deficits^{22, 28}. The milder cognitive deficit evidenced in patients with atypical deletions from the present series is consistent with this hypothesis. However, the presence of some aspects of the characteristic WBS cognitive profile indicates that one should be cautious in drawing firm conclusions on genotype/phenotype correlation from a limited number of subjects all bearing different microdeletions (Figure 3B). This notion is further emphasized by the identification of unusually highly functioning patient that carries the classical deletion²⁵ and by a family with a balanced translocation t(7;16)(q11.23;q13) within the elastin gene associated with variable expression of the WBS phenotype³⁰. Interestingly, both our atypical patients and none of the previously described patients with similar partial deletions^{22, 23, 27, 28} showed the facial features characteristic of WBS, suggesting that hemizyosity of genes mapping to the telomeric end of the common deletion might be involved. An additional aspect which can be putatively linked with hemizyosity of telomeric genes is premature aging, since this feature was absent in IM3 at age 30.

Phenotype/genotype correlation is one of the major challenges in clinical human genetic of contiguous gene syndromes. The techniques used in this report, in particular QPCR are suitable to map precisely any aneuploidy, thus giving a reliable means to perform large-scale diagnosis to detect uncommon patients, with a fast reporting time and at a reasonable cost.

Acknowledgments

We thank P. Descombes, M. Docquier, M. Gagnebin, C. Ucla and C. Wyss for assistance and discussions. This work was supported by grants from the Jérôme Lejeune Foundation, Telethon Action Suisse, the Désirée and Niels Yde Foundation and the Swiss National Science Foundation to AR and from the Italian Minister of Health "Ricerca Corrente" 2005 to GM.

Licence for Publication

The Corresponding Author has the right to grant on behalf of all authors and does grant on behalf of all authors, an exclusive licence (or non exclusive for government employees) on a worldwide basis to the BMJ Publishing Group Ltd and its Licensees to permit this article (if accepted) to be published in JMG editions and any other BMJ PGL products to exploit all

subsidiary rights, as set out in our licence (<http://jmg.bmjournals.com/misc/ifora/licenceform.shtml>)."

Competing interests

The authors declare no competing interests.

Figure Legends:

Figure 1 Diagnosing WBS by paralogous sequence quantification

Distribution of the relative abundancies of the query chromosome upon combination of the CYLN2 and the WBSR3.4M assays. Control samples are in burgundy and WBS patients in purple. The positions of samples corresponding to the two patients carrier of an atypical deletion (CO3 and IM3), i.e. euploid for the CYLN2 and WBSR3.4M assays are indicated by asterisks.

Figure 2 Diagnosing WBS by real-time quantitative PCR (QPCR)

Means and standard deviations of real-time quantitative PCR results obtained for 11 assays from the 7q11.23 region with 61 controls (burgundy square) and 92 WBS patients (purple disks) DNAs. The extension of the classical deletion observed in WBS (double-head black arrow) and the location of the Low-Copy Repeats (LCRs; green arrow, BLOCK C; yellow arrow, BLOCK A; red arrow, BLOCK B; ³¹) are indicated.

Figure 3 Atypical deletions

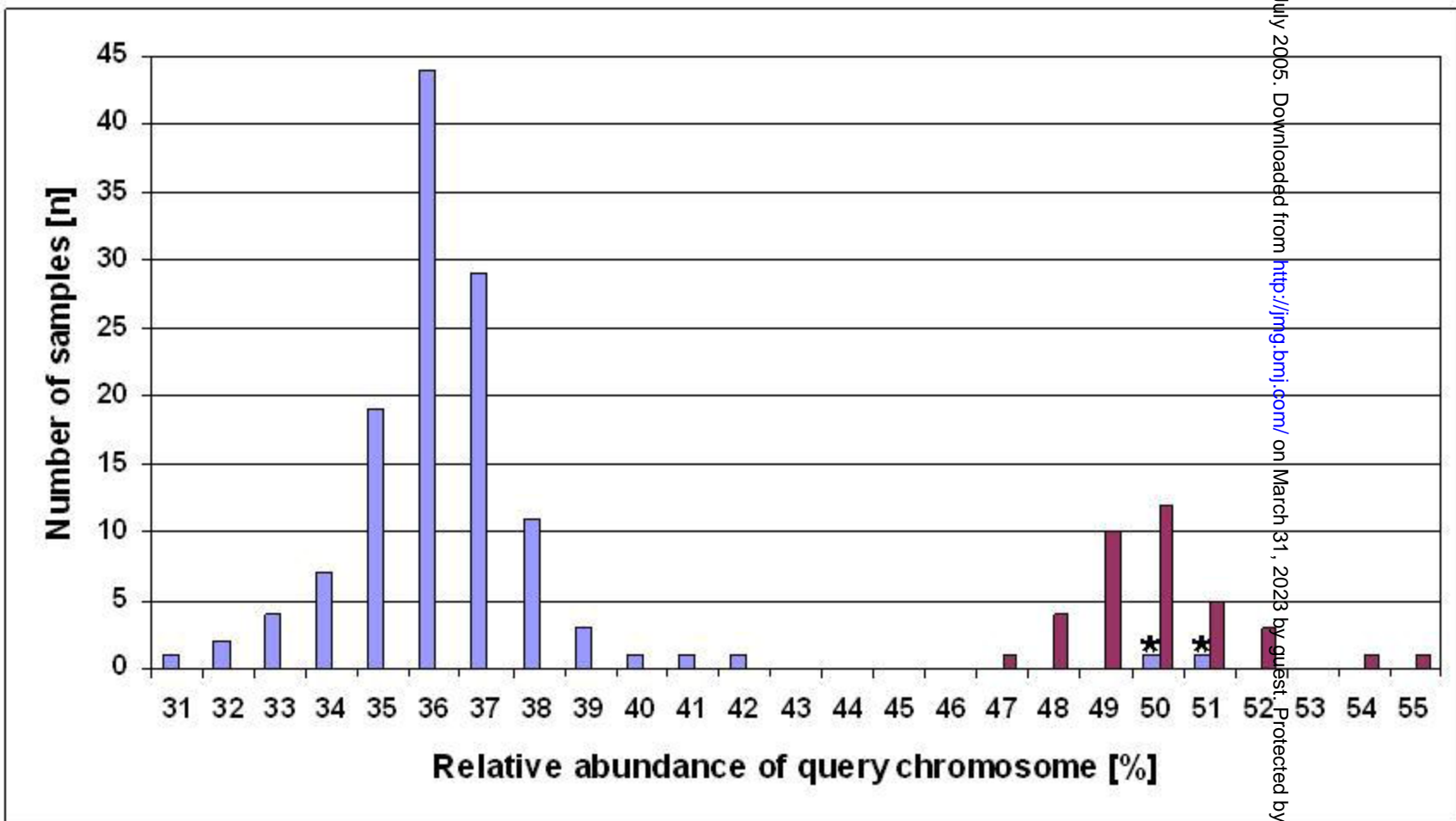
(A) Typical real-time quantitative PCR results obtained for a control (burgundy squares) and a typical WBS patient (purple disks) sample besides the samples of atypical patients CO3 (dark blue disks) and IM3 (red disks).

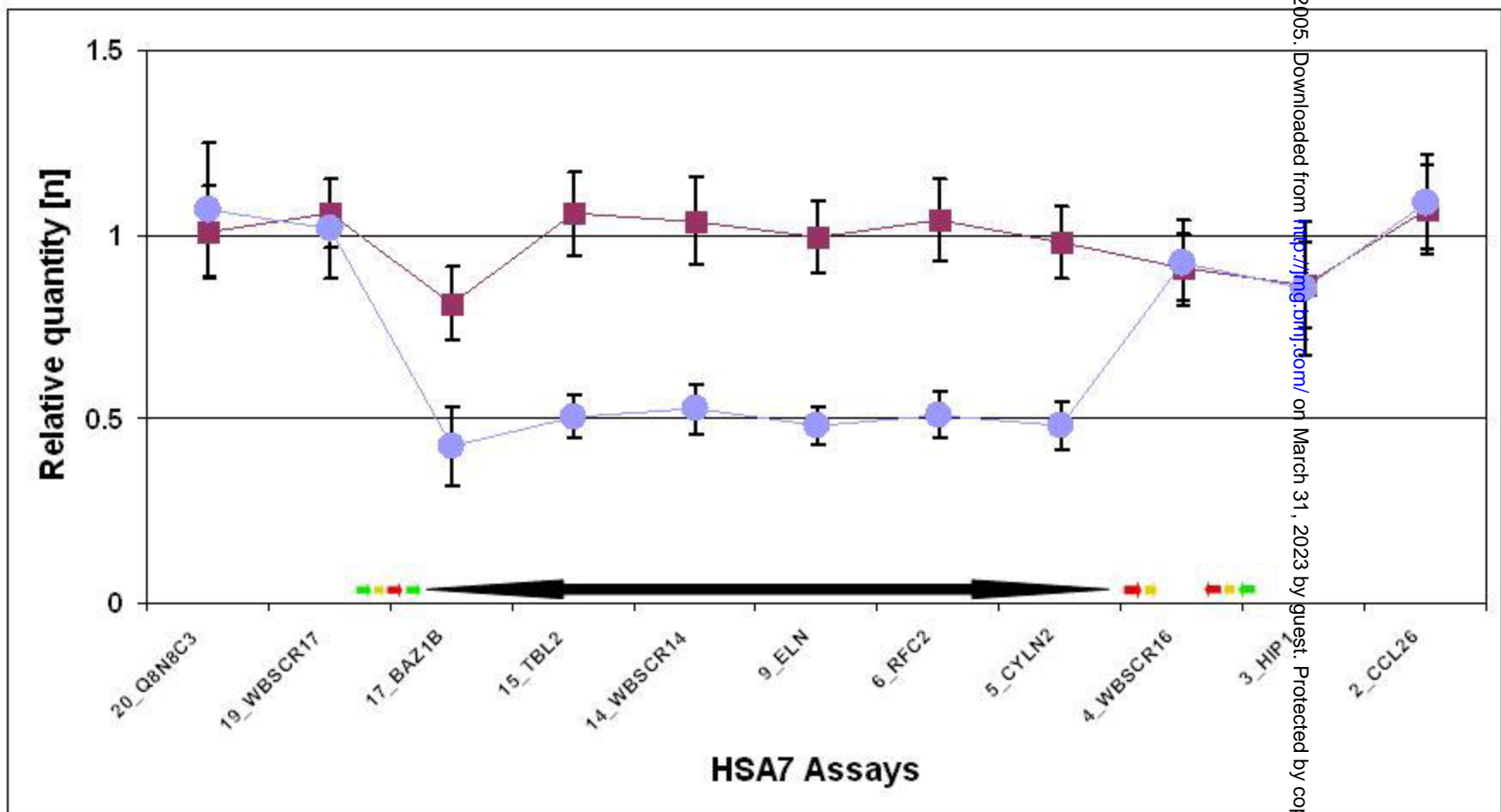
(B) Schematic partial transcript map of the WBS critical region. Single copy transcripts mapping to the WBS critical region are represented by blue boxes, whereas duplicons within the Low-Copy Repeats are depicted by colored arrows (BLOCK A: yellow; BLOCK B: red; BLOCK C: green; ³¹). The name of the hemizygous and normal-copy genes are printed diagonally and vertically, respectively. The extent of the deletion observed in classical WBS (short and long deletions), as well as in the atypical patients discussed in this manuscript are denoted by grey boxes below the transcript map. Unclear deletion statuses are represented by white boxes. Patients symbols and references are indicated on the right.

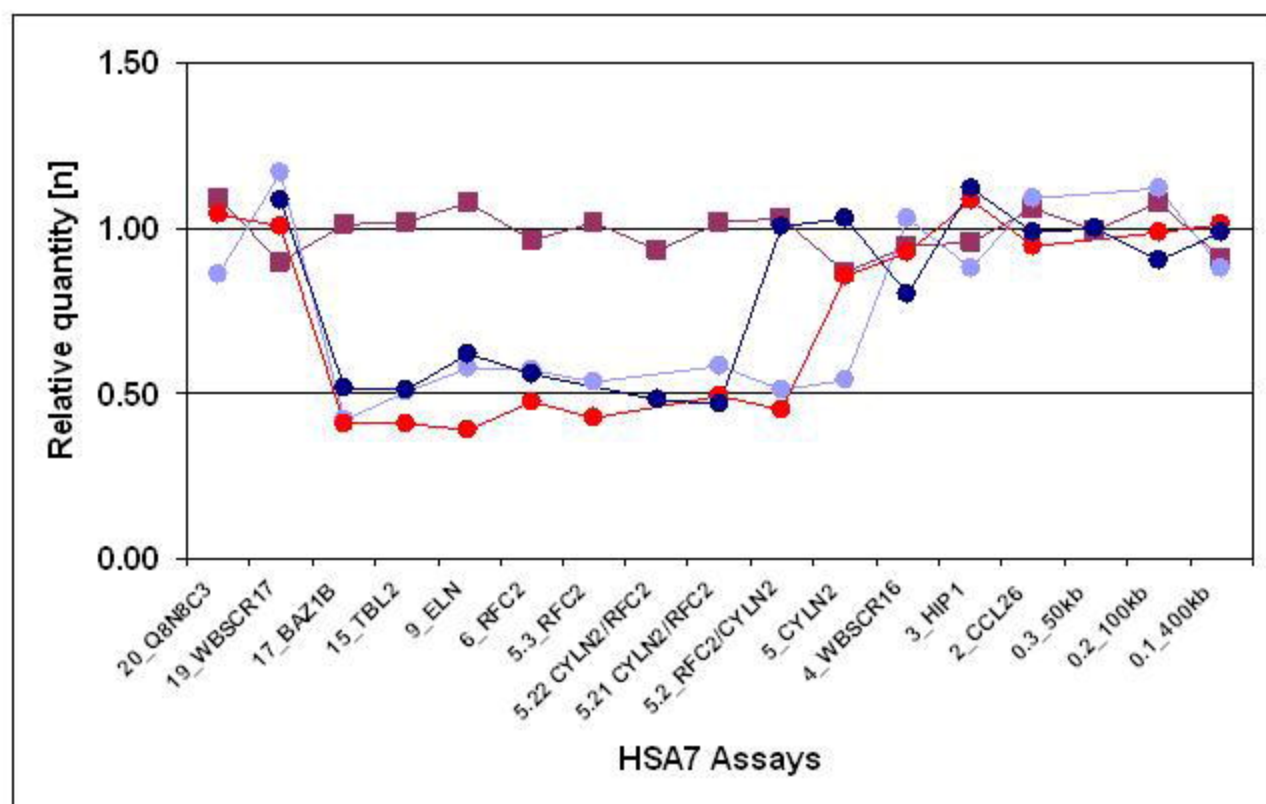
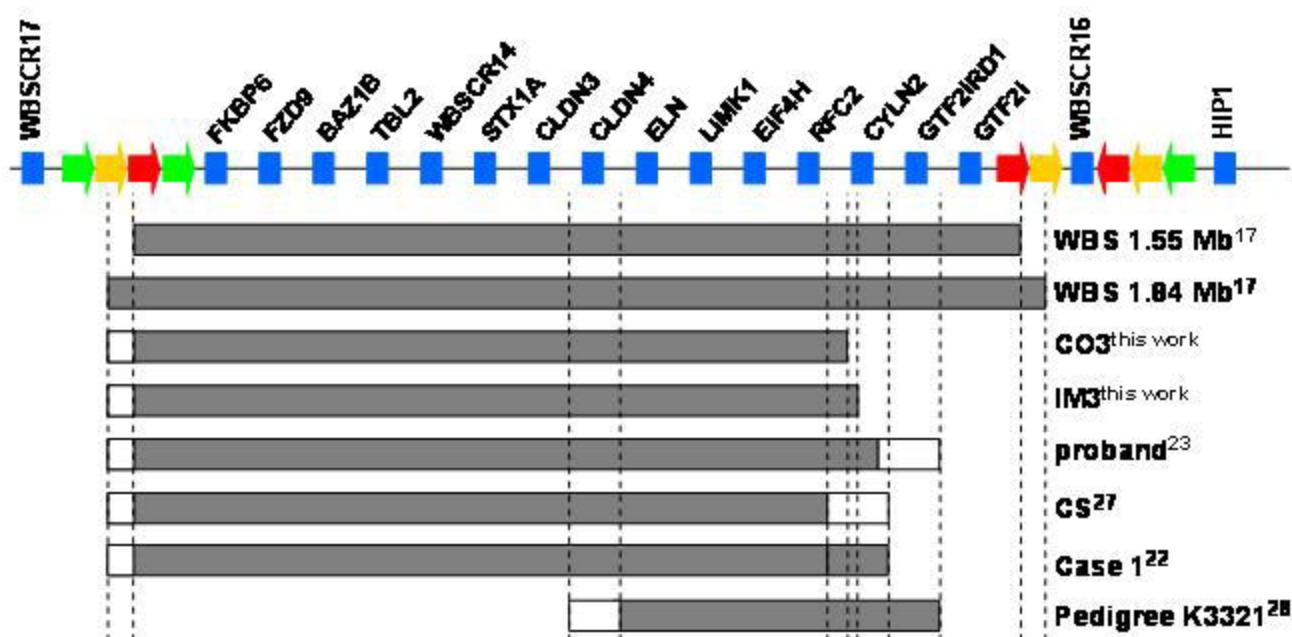
Bibliography

1. Lowery MC, Morris CA, Ewart A, *et al.* Strong correlation of elastin deletions, detected by FISH, with Williams syndrome: evaluation of 235 patients. *Am J Hum Genet* 1995;**57**(1):49-53.
2. Bonnet D, Cormier-Daire V, Kachaner J, *et al.* Microsatellite DNA markers detects 95% of chromosome 22q11 deletions. *Am J Med Genet* 1997;**68**(2):182-4.
3. Lander ES, Linton LM, Birren B, *et al.* Initial sequencing and analysis of the human genome. *Nature* 2001;**409**(6822):860-921.
4. Venter JC, Adams MD, Myers EW, *et al.* The sequence of the human genome. *Science* 2001;**291**(5507):1304-51.
5. Consortium IHG. Finishing the euchromatic sequence of the human genome. *Nature* 2004;**431**(7011):931-45.
6. Ewart AK, Morris CA, Atkinson D, *et al.* Hemizyosity at the elastin locus in a developmental disorder, Williams syndrome. *Nat Genet* 1993;**5**(1):11-6.
7. Stromme P, Bjornstad PG, Ramstad K. Prevalence estimation of Williams syndrome. *J Child Neurol* 2002;**17**(4):269-71.
8. Francke U. Williams-Beuren syndrome: genes and mechanisms. *Hum Mol Genet* 1999;**8**(10):1947-54.
9. Osborne LR. Williams-Beuren syndrome: unraveling the mysteries of a microdeletion disorder. *Mol Genet Metab* 1999;**67**(1):1-10.
10. Morris CA, Demsey SA, Leonard CO, *et al.* Natural history of Williams syndrome: physical characteristics. *J Pediatr* 1988;**113**(2):318-26.
11. Bellugi U, Bihrlle A, Jernigan T, *et al.* Neuropsychological, neurological, and neuroanatomical profile of Williams syndrome. *Am J Med Genet Suppl* 1990;**6**:115-25.
12. Cherniske EM, Carpenter TO, Klaiman C, *et al.* Multisystem study of 20 older adults with Williams syndrome. *Am J Med Genet* 2004;**131A**(3):255-64.
13. Deutsch S, Choudhury U, Merla G, *et al.* Detection of aneuploidies by paralogous sequence quantification. *J Med Genet* 2004;**41**(12):908-915.
14. Higuchi R, Fockler C, Dollinger G, *et al.* Kinetic PCR analysis: real-time monitoring of DNA amplification reactions. *Biotechnology (N Y)* 1993;**11**(9):1026-30.
15. Higuchi R, Dollinger G, Walsh PS, *et al.* Simultaneous amplification and detection of specific DNA sequences. *Biotechnology (N Y)* 1992;**10**(4):413-7.
16. Vandesompele J, De Preter K, Pattyn F, *et al.* Accurate normalization of real-time quantitative RT-PCR data by geometric averaging of multiple internal control genes. *Genome Biol* 2002;**3**(7):RESEARCH0034.
17. Bayes M, Magano LF, Rivera N, *et al.* Mutational mechanisms of Williams-Beuren syndrome deletions. *Am J Hum Genet* 2003;**73**(1):131-51.
18. Liu DP, Schmidt C, Billings T, *et al.* Quantitative PCR genotyping assay for the Ts65Dn mouse model of Down syndrome. *Biotechniques* 2003;**35**(6):1170-4, 1176, 1178 passim.
19. Merla G, Ucla C, Guipponi M, *et al.* Identification of additional transcripts in the Williams-Beuren syndrome critical region. *Hum Genet* 2002;**110**(5):429-38.
20. Antonarakis SE, Lyle R, Dermitzakis ET, *et al.* Chromosome 21 and down syndrome: from genomics to pathophysiology. *Nat Rev Genet* 2004;**5**(10):725-38.
21. Botta A, Novelli G, Mari A, *et al.* Detection of an atypical 7q11.23 deletion in Williams syndrome patients which does not include the STX1A and FZD3 genes. *J Med Genet* 1999;**36**(6):478-80.

22. Hirota H, Matsuoka R, Chen XN, *et al.* Williams syndrome deficits in visual spatial processing linked to GTF2IRD1 and GTF2I on chromosome 7q11.23. *Genet Med* 2003;**5**(4):311-21.
23. Gagliardi C, Bonaglia MC, Selicorni A, *et al.* Unusual cognitive and behavioural profile in a Williams syndrome patient with atypical 7q11.23 deletion. *J Med Genet* 2003;**40**(7):526-30.
24. Heller R, Rauch A, Luttgen S, *et al.* Partial deletion of the critical 1.5 Mb interval in Williams-Beuren syndrome. *J Med Genet* 2003;**40**(8):e99.
25. Karmiloff-Smith A, Grant J, Ewing S, *et al.* Using case study comparisons to explore genotype-phenotype correlations in Williams-Beuren syndrome. *J Med Genet* 2003;**40**(2):136-40.
26. Korenberg JR, Chen XN, Hirota H, *et al.* VI. Genome structure and cognitive map of Williams syndrome. *J Cogn Neurosci* 2000;**12 Suppl 1**:89-107.
27. Tassabehji M, Metcalfe K, Karmiloff-Smith A, *et al.* Williams syndrome: use of chromosomal microdeletions as a tool to dissect cognitive and physical phenotypes. *Am J Hum Genet* 1999;**64**(1):118-25.
28. Morris CA, Mervis CB, Hobart HH, *et al.* GTF2I hemizyosity implicated in mental retardation in Williams syndrome: genotype-phenotype analysis of five families with deletions in the Williams syndrome region. *Am J Med Genet* 2003;**123A**(1):45-59.
29. Tassabehji M. Williams-Beuren syndrome: a challenge for genotype-phenotype correlations. *Hum Mol Genet* 2003;**12 Spec No 2**:R229-37.
30. Duba HC, Doll A, Neyer M, *et al.* The elastin gene is disrupted in a family with balanced translocation t(7;16)(q11.23; q13) associated with a variable expression of the Williams-Beuren syndrome. *Eur J Hum Genet* 2002;**10**:351-361.
31. Valero MC, de Luis O, Cruces J, *et al.* Fine-scale comparative mapping of the human 7q11.23 region and the orthologous region on mouse chromosome 5G: the low-copy repeats that flank the Williams-Beuren syndrome deletion arose at breakpoint sites of an evolutionary inversion(s). *Genomics* 2000;**69**(1):1-13.





A**B**

Supplementary Online Material

Howald et al.

Supplementary Figure Legends

Supplementary Figure S1

Alignment of genomic sequences from the BAZ1B region with its paralogous sequence from HSA10 (accession: NT_030059.10|Hs10_30314). The sequences corresponding to the PCR amplification primers and the pyrosequencing primer are highlighted in yellow and blue, respectively. The analyzed PSM is marked in black

Supplementary Figure S2

Alignment of genomic sequences from the CYLN2 and WBSCR3.4M region with its paralogous sequence from HSA2 (accession: NT_005403.13|Hs2_5560). The sequences corresponding to the PCR amplification primers are highlighted in red and yellow, while the pyrosequencing primers are highlighted in purple and blue. The analyzed PSMs are marked in black.

Supplementary Figure S3

Diagnosing WBS by paralogous sequence quantification

Typical results (pyrograms and percentage of both Paralogous Sequence Mismatches) of controls (left column) and WBS patients (right column) for all the assays. The name of each assay and the analyzed sequence are indicated on the left. The expected results for euploidy at this marker are indicated by histograms below the pyrograms.

Supplementary Figure S4

Diagnosing WBS by real-time quantitative PCR (QPCR)

Typical results of the real-time quantitative PCR-approach to diagnose the extension of the 7q11.23 deletion in four WBS patients (disks) and four controls (square). The extension of the classical deletion observed in WBS (double-head black arrow) and the location of the Low-Copy Repeats (LCRs; green arrow, BLOCK C; yellow arrow, BLOCK A; red arrow, BLOCK B; (Valero et al., 2000) are indicated.

Figure S1

```
BAZ1B: 5483   gagagcggcagagaagctctgagagccccttcccacacaacaatctagctctagttgtt 5542
|||||
HSA10: 6205598 gagagcggcagagaagctctgagagcccctt--cccacacaacaatctagttctagttgtt 6205541

BAZ1B: 5543   atatttaggcaaaactttgtagtcttcctttcccttttatgatggatgataaaaagtac 5602
|||||
HSA10: 6205540 atatttaggcaaaactttgtagtcttcctttcccttttatgatggatgataaaa-tac 6205482

BAZ1B: 5603   aaaacagggtttttctttt--ttatcacctttgaatttggaattttgagcacccaagctc 5661
|||||
HSA10: 6205481 aaaacagcg-tttaattttcttatcacctttgaatttggaattttgagcacccaagctc 6205423

BAZ1B: 5662   ttctgtaccta--t---ttaaagtcaccaaggggactgca gctcctagaacatgagaat 5716
|||||
HSA10: 6205422 ttctgtacctatttaaattaaagtcaccaaggggactgca gctcctagaacatgagaat 6205363

BAZ1B: 5717   caagcctctt
|||||
HSA10: 6205362 caagcctctc
```

Figure S2

```
CYLN2: 32178   ccaactggaagatttccacctggagtgctttccacatgg-gccccaaggagg-tgtct 32235
|||||
HSA2 : 56277718 ccaactggaagatttccacctggagtgctgggt--a-atggaacccaaggaggct-tct 56277663

CYLN2: 32236   ttctc--tctttctgccaggctctgaagaggcagaggaggcaggggaggtctccaggct 32293
|||||
HSA2 : 56277662 ttctcgtctctttctgctgggctctgaagaggcagaggaggcaggggaggt--ctccaggct 56277605

CYLN2: 32294   ttggggccgtgacagcagct-tgggtctctcctgcttcca caggtacttccagtgccac 32352
|||||
HSA2 : 56277604 gtggggccatgacagcag-tgtgagctctcctgcttcca caggtacttccagtgccac-g 56277547

CYLN2: 32353   ccaagtttgtctcttcgcgccatccacaaagtgatccgta-tcggttcccatctacc 32411
|||||
HSA2 : 56277546 ccaagtttgtctctttgcatccatccacaaggtgatccatact-gggttcccatccacc 56277488

CYLN2: 32412   agccca gccaaggccaagaagaccaagcgtatgcccattgggtgtgtc agcaactgaccac 32471
|||||
HSA2 : 56277487 agccca gccaaggccaagaagaccaaacgtatgcccattgggtgtgtc agcaactgaccac 56277428

CYLN2: 32472   agtcccagcagttcctccatcagctccgtcagctctgtggcctcctccgt-ggggggtcg 32530
|||||
HSA2 : 56277427 agtcccagcatttctccatcagttccatcggttccatggcctcctttgtagggggg-cg 56277369

CYLN2: 32531   gcc 32533
|||
HSA2 : 56277368 gcc 56277366
```

Figure S3

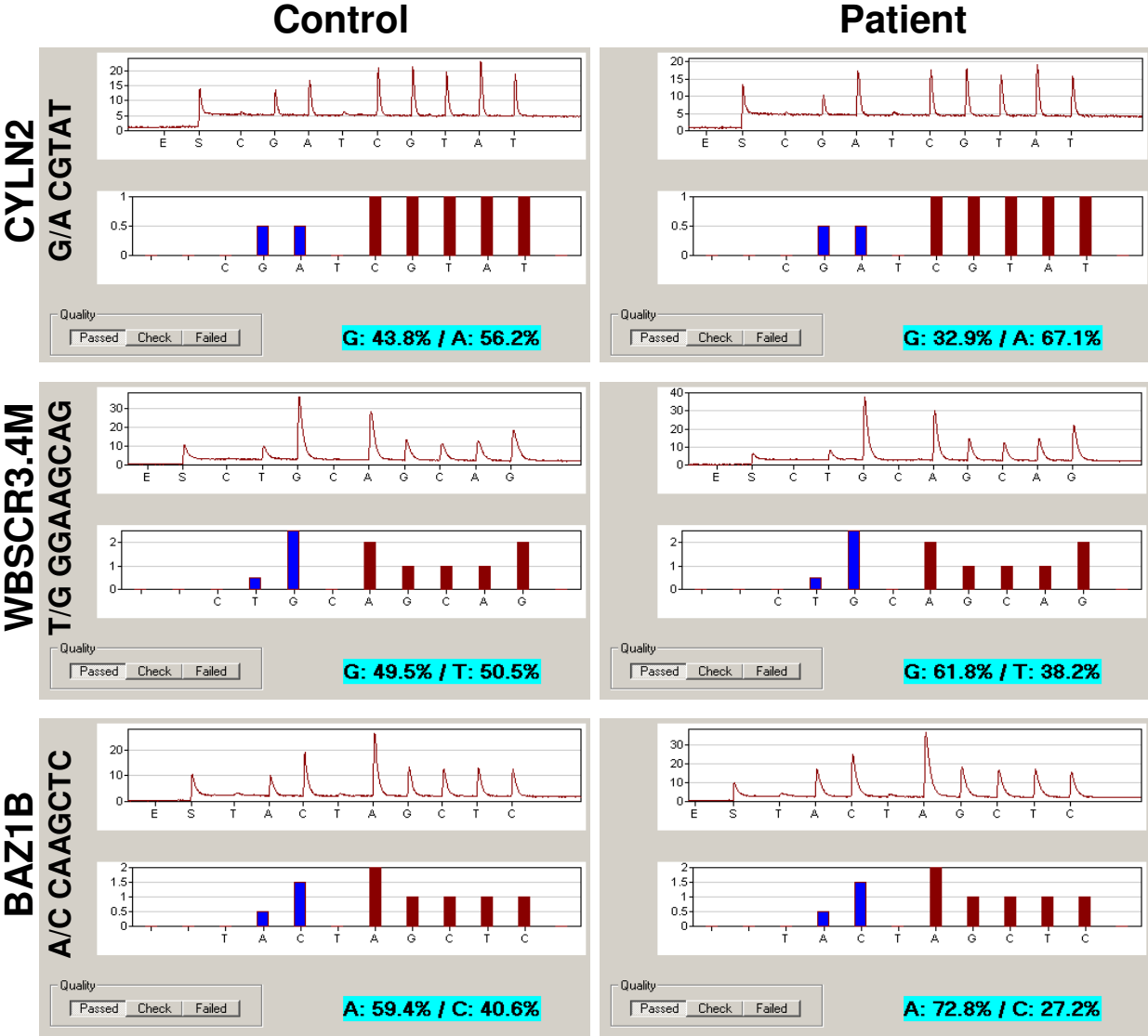


Figure S4

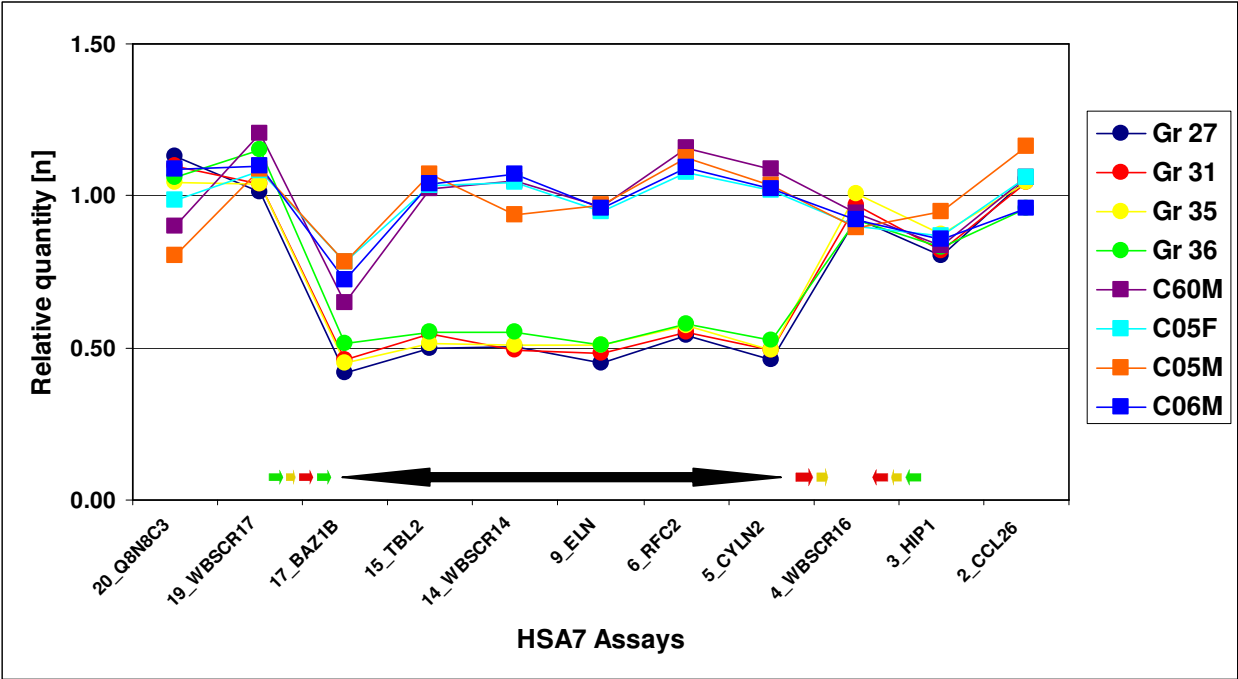


Table S1

TableS1: Primers and conditions used to diagnose WBS by Paralogous Sequence Quantification

Assay	Primers			Conditions				Amplification ¹	
	ID	Sequence	Role	MgCl ₂	DMSO	Buffer	Polymerase	TD, 10 cycles	PCR, 30 cycles
BAZ1B	14748-BAZ1B(new)Fw py	GGCAAACCTTTGTAGTCTTC	Forward primer	0 mM	5%	1 x Taq buffer	Taq	95° 30", 63-58.5° 30", 72° 20"	95° 30", 58° 30", 72° 20"
	14750-BAZ1B (new)Rv py	7GATTCTCATGTTCTAGGAGC	Reverse primer						
	14749-BAZ1B(new)SNP py	TTGAAATTTTGAGCAC	Pyrosequencing primer						
CYLN2	13036Cynl2_WBSF	GCCAAGGCCAAGAAG	Forward primer	1.5 mM	5%	1 x Taq buffer	Taq	95° 30", 63-58.5° 30", 72° 20"	95° 30", 58° 30", 72° 20"
	13037Cynl2_WBSR	7GGGACTGTGGGTCAGTGCT	Reverse primer						
	13038Cynl2_WBSS	CCAAGAAGACCAA	Pyrosequencing primer						
WBSR3.4	14754-WBSR3.4(SNP M)	7AAGATTTCCACCTGGAGTG	Forward primer			1 x RED-7Taq buffer	Jumpstart RED-7Taq	95° 30", 58-53.5° 30", 72° 20"	95° 30", 53° 30", 72° 20"
	14755-WBSR3.4(SNP M)	TCACCCATGGCCATAC	Reverse primer						
	14756-WBSR3.4(SNP M)	GGCACTGGAAGTACCTG	Pyrosequencing primer						

¹The amplification process begins with 5' at 95° and ends with 3' elongation at 72°

Table S2

TableS2: Primers used to diagnose WBS by quantitative PCR

Assay	Forward primer		Reverse primer		mapping to HSA7 bp
	ID	Sequence	ID	Sequence	
2_CCL26	15428_2_CCL26F	TTTGATCATAACAGCAAGCCAGGA	15429_2_CCL26R	CCCCAGTTCCTGCTGTG	75017006
3_HIP1	15430_3_HIP1F	GTGCCACAGGTCATCCC	15431_3_HIP1R	AACCTGGAAGTCCTGGTTTGAA	74974601
4_WBSR16	15432_4_WBSR16F	CATGCTTTGTGGAACTGCTT	15433_4_WBSR16R	AGAGGACAGCAGTGAATCCA	73898628
5_CYLN2	15434_5_CYLN2F	CTGCTCTTCTCCTGTGGCT	15435_5_CYLN2R	AGCTGTTGCCAGGTCTCT	73169734
6_RFC2	15436_6_RFC2F	TGACAACCCCTTGCCAC	15437_6_RFC2R	TGCCATATTTGGTAATGCGC	73067913
9_ELN	15442_9_ELN	GGCATGAGACGCTCCACAT	15443_9_ELN	TTCTGAGCAGGGCAACAC	72865074
10_CLDN4	15444_10_CLDN4F	AACACAGGTGGACCATGCTAGA	15445_10_CLDN4R	GGATCTGTGACCCGGCTAATG	72655622
11_WBSR21	15446_11_WBSR21F	CAGCTGGGTGGAGCAAGC	15447_11_WBSR21R	AGGGAGTGCCTTGTCTGGG	72561409
14_WBSR14	15452_14_WBSR14F	CACGCAATTTCTGATCCATT	15453_14_WBSR14R	GCAGGCGGTTGCGC	72450358
15_TBL2	15454_15_TBL2F	CTGTCTGTCACTAGCCTCTGCA	15455_15_TBL2R	CCAGGCCCTCGGCA	72408518
17_BAZ1B	15458_17_BAZ1BF	AGTTACTTCCGCTTTGAATTTGG	15459_17_BAZ1BR	GGCAACTTCCACACAAAACC	72339015
19_WBSR17	15462_19_WBSR17F	AAAATCTCCTTCTGGCCCC	15463_19_WBSR17R	TTGCCTAGCACAACCCCC	70206028
20_Q8N8C3	15464_20_Q8N8C3F	CGCAGCTTGCTTCTTAGCTT	15465_20_Q8N8C3R	AGGCTGAGTTTCTGACTTGC	70012994
17.1_BAZ1B	15610_17.1_BAZ1B FW	CGCTGTGGCCAGATAGCAT	15843_17.1_BAZ1B RW	CACCATGGAGGGCATCAA	72269607
16.1_BCL7B	15611_16.1_BCL7B FW	AGGCGTGCACAGGCTATCA	15844_16.1_BCL7B RW	CTCCCTGGCTCGCATAGGT	72368450
5.3_RFC2	15617_5.3_RFC2 FW	GGATGGTGAAGCCCTGGTT	15850_5.3_RFC2 RW	GGTTGCCATCATCTGGTTTG	73076964
5.2_RFC2/CYLN2	15618_5.2_RFC2/CYLN2 FW	ACTCATGACACACCCGGCTTTC	15851_5.2_RFC2/CYLN2 RW	CAAGCTGCTCTCTCAAGTTT	73103486
4.1_GTF2IRD1	15862_4.1_GTF2IRD1 Fw	GAGGGCTCAGCCCCATA	15854_4.1_GTF2IRD1 RW	AATGGGAGGACGACACCA	73362277
21_100kb outWBScentro	15622_21_100kb outWBScentro FW	CAAACCGCTGTCCATTACAGAA	15855_21_100kb outWBScentro RW	ATGTCAGACTGGGCTCATCAGA	69919994
22_200Kb outWBScentro	15623_22_200Kb outWBScentro FW	GCCTAAAGTCTTGGCAACAG	15856_22_200Kb outWBScentro RW	TCTCCCCAACACCATGGT	70254521
23_400Kb outWBScentro	15624_23_400Kb outWBScentro FW	AAGGGATGCTTGAAGGCTGTATG	15857_23_400Kb outWBScentro RW	GGAGAAAACCTAGCCCGATT	69619016
0.3_50Kb outWBSstelo	15625_0.3_50Kb outWBSstelo FW	TGGCGTCCAAGCAATCCT	15858_0.3_50Kb outWBSstelo RW	GCCAGACAAGCCAGGTAGA	74799070
0.2_100Kb outWBSstelo	15626_0.2_100Kb outWBSstelo FW	CCCCAAGCAACACTTGATCA	15859_0.2_100Kb outWBSstelo RW	TGGGCCCAAAACCATAGAG	74850630
0.1_400Kb outWBSstelo	15627_0.1_400Kb outWBSstelo FW	CACCAAGACTGGCGTTTCC	15860_0.1_400Kb outWBSstelo RW	GCGGACCAAGATTTCTGAC	75207763
5.22_CYLN2/RFC2	15999_5.22_CYLN2/RFC2 F	GGGCATTTGGCCAGAGATG	16000_5.22_CYLN2/RFC2 R	CCTTCCAGGCAAGCCAAAT	73085743
5.21_CYLN2/RFC2	16001_5.21_CYLN2/RFC2 F	GGGCACCCCGAGGTATG	16002_5.21_CYLN2/RFC2 R	CAGATTTGAAGCTGAGCTTGCT	73090411
4.01_WBSR16	16003_4.01_WBSR16 F	TTGAACCTCAGGCAAAAGG	16004_4.01_WBSR16 R	CTTTTAGGCCACAAAAGCATCTT	73897993
4.02_WBSR16	16005_4.02_WBSR16 F	GCTTGATCGATTGAGCCACAT	16006_4.02_WBSR16 R	CTTGAGCAATCCCAGTCTGTG	73894413
15.1_TBL2	17741_15.1_TBL2 F	ACAGGACCCCTCCGCATACT	17742_15.1_TBL2 R	TTTGCCCCACCAATT	72386418
14.3_TBL2	17743_14.3_TBL2 F	CTCTGACTGACCCGCTCCTT	17744_14.3_TBL2 R	GGCCCGAGAAAACCCAGAA	72414194
14.1_WBSR14	17745_14.1_WBSR14 F	CAGGAGAGACCACCGCAGTATT	17746_14.1_WBSR14 R	CCTCTCCTGCTTGGATGAA	72440902
14.2_WBSR14	17747_14.2_WBSR14 F	GACGGCAGGAGGATGATG	17748_14.2_WBSR14 R	GAGAGAGGGAGTGCAGTACATTTA	72424335
4.3_CYLN2	17749_4.3_CYLN2 F	GACCCCTATATCCGGGAGTAG	17750_4.3_CYLN2 R	TGGCCAGAGTGATGCTTTTATC	73225057
5.01_CYLN2	17751_5.01_CYLN2 F	GCCTGGGAGGCATGCTT	17752_5.01_CYLN2 R	CAGGGACATGAACCCGAAGA	73119253
normalization 21-1	13384hsacgh-21-1A	TCTCGATTCCITTAGGCTCAACT	13385hsacgh-21-1B	GCTCAGCTCAGGATGCAGAAA	HSA21_14781146
normalization 21-3	13388hsacgh-21-3A	CCACCTCAAGTATACCGAAGTCCCTA	13389hsacgh-21-3B	GGAAAGCGCTGATGTGAA	HSA21_21589275
normalization 21-4	13390hsacgh-21-4A	CAATTGAGGTCAGGTGATACTCAGTAA	13391hsacgh-21-4B	GCCAGGTTTGAATGTTTGTCTAAGTC	HSA21_24204262
normalization 21-6	13394hsacgh-21-6A	CGTCACATCAGATCTCACTATTG	13395hsacgh-21-6B	ACCACGTGAAAGGAGGTTTCC	HSA21_30761032